University of Huddersfield Repository

Zhen, Dong, Shi, Zhanqun, Song, Zhongyue, Gu, Fengshou and Ball, Andrew

Combustion Noise Analysis for Combustion and Fuels Diagnosis of a CI Diesel Engine Operating with Biodiesels

Original Citation

Zhen, Dong, Shi, Zhanqun, Song, Zhongyue, Gu, Fengshou and Ball, Andrew (2015) Combustion Noise Analysis for Combustion and Fuels Diagnosis of a CI Diesel Engine Operating with Biodiesels. Combustion Science and Technology. p. 150707092649006. ISSN 0010-2202

This version is available at http://eprints.hud.ac.uk/25060/

Combustion Noise Analysis for Combustion and Fuels Diagnosis of a CI Diesel Engine Operating with Biodiesels

Dong Zhen[1*], Zhanqun Shi[1], Zhongyue Song[1], Fengshou Gu[2] and Andrew Ball[2]

[1.] School of Mechanical Engineering, Hebei University of Technology, Tianjin, 300130, China

[2.] Centre for Efficiency and Performance Engineering, University of Huddersfield, Huddersfield, HD1 3DH, U.K

* Corresponding author: Tel.: +86 022 26582598, Email: D.Zhen@hebut.edu.cn

Abstract

In this paper, the combustion noise of a compression ignition (CI) diesel engine operating with biodiesels has been investigated experimentally. It aims to explore an effective method for combustion process monitoring and fuel quality evaluation through analysing the characteristics of the engine combustion noise. The experiments were conducted on a four-cylinder, four-stroke, direct injection and turbocharged diesel engine fuelled with biodiesels (B50 and B100) and normal pure diesel, and operating under different loads and speeds. The signals of cylinder head vibration, engine noise and in-cylinder pressure were measured during the tests. A coherent power spectrum analysis method was used to investigate the vibration and noise signals that related to the combustion process. The results shown that the noise components at the frequency band of 2 -3 kHz are closely related to the combustion process. Subsequently, the Wigner-Ville distribution is employed to present the energy distribution of engine noise in the time-frequency domain. Then a band-pass filter based on fractional Fourier transform (FRFT) is developed to extract the main component of the combustion noise for feature extraction. The results show that the sound pressure levels (SPLs) of the extracted combustion noise of the test diesel engine fuelled with biodiesels are higher than that fuelled with diesel. This is also identical to the variation of in-cylinder pressure. The results demonstrate that the features of the extracted combustion noise can indicate the combustion characteristics and provide useful information for monitoring the combustion process and evaluating the fuel quality of diesel engines.

Key words: Combustion noise; Diesel engine; Biodiesels; fractional Fourier transform.

1. Introduction

The demand for using petroleum-based fuel has gradually been increased in numerous areas with the development of industrial application. However, the resources of petroleum-based fuel are non-renewable and the remaining global ones are sufficient to meet demand up to 2030 (Kjärstad and Johnsson, 2009). Therefore, a demand to develop alternative fuels which are cheaper and environmentally acceptable has been considered to reduce the dependency on fossil fuel due to the limited resources (Aydin and Bayindir, 2010). It pointed out that biodiesel is one of the most promising renewable, alternative and environmentally fuels, and can be used in diesel engines directly (Aydin and Bayindir, 2010)(Hazar, 2009). However, the diesel engines are not specifically designed for biodiesel supplied. How the performance, emission and noise characteristics of diesel engines will be when using biodiesel as the fuel supply has been a popular research topic.

The researchers are not only focus on the study of engine performance assessment, but also investigate the combustion process and emission characteristics of diesel engines fuelled with biodiesel (Enweremadu and Rutto, 2010)(Aydin and Bayindir, 2010)(Hazar, 2009)(Murillo et al., 2007)(Tesfa et al., 2013)(Tesfa et al., 2012)(Dorado et al., 2003). Dorado et al. (Dorado et al., 2003) studied the effect of used olive oil methyl ester on combustion efficiency using a DI diesel Perkins engine, and concluded that biodiesel provided more oxygen for combustion as a result of its oxygen concentration increased. Sudhir et al. (Sudhir et al., 2007) investigated the engine performance on a single-cylinder, four-stroke, direct injection, water-cooled diesel engine test rig. The test was conducted at various loads from no load condition to the rated full load using diesel, fresh oil and waste cooking oil. Results showed that the pure waste cooking oil was only poorer at part loads compared to diesel fuel performance. Hamasaki et al. (Hamasaki et al., 2001) tested the emission of a single-cylinder engine at high speed and different loads with diesel fuel and three biodiesel fuels from used cooking oil. The acid values of the biodiesel were different. Results showed that CO emissions were increased as the acid value was increased while NOx emissions were slightly decreased at low loads but increased at high loads.

Beside the study of combustion, emission and engine performance characteristics of diesel engines running with biodiesels, many researchers also carried out the investigation of engine noise characteristics (Shu et al., 2004)(Shu and Liang, 2007)(Priede, 1980)(LI et al., 2001)(Pruvost et al., 2009)(Ra et al., n.d.)(Priede, 1979)(Brunt et al., 1998). Shu and Liang (Shu and Liang, 2007) analysed the complex engine noises using coherent power spectrum technology, and found that the engine noise at the low frequency band are the primarily resources of machinery noise, in contrast to combustion induced noise are mainly located in the high frequency band. Li and Gu (LI et al., 2001) analysed engine acoustic signals by employed independent component analysis (ICA) to identify the engine noise sources, and concluded that the ICA is powerful in the retrieval of engine noise sources such as combustion and valve operations, but the ICA to other mechanical signals is limited due to its non-Gaussian restriction on the sources. Pruvost (Pruvost et al., 2009) developed an improved spectrofilter to separate diesel engines combustion and mechanical noise. Based on theoretical and experimental study, Pruvost found that the combustion and mechanical noises are similar levels, highly correlated and overlapped in both the time and frequency domains, and the improved spectrofilter is enable to separate the two noises through computing upon the residual part of the signals.

As stated by the literatures, diesel engines produce a complex noise whose level and sound quality both strongly depend on the fuel combustion (Shu et al., 2004). Therefore, it is possible to analyse the combustion noise characteristics for combustion monitoring and fuel quality evaluation. Based on the working principle of diesel engines, the combustion noise occurs towards the end of the compression strokes and subsequent expansion strokes. The change of cylinder pressure causes the vibration of the engine components such as the cylinder head, pistons, connecting rods and engine body. All the vibration induced noises contributes to the overall engine noise level (LI et al., 2001). The vibration and noise of diesel engines are generated due to the variation of the cylinder pressure which is related to the engine combustion process. Actually, the unpleasant noise signature of diesel engines is due to the harsh irregular self-ignition of the fuel (Pruvost et al., 2009). Therefore, the fuel quality could be evaluated by

analysing the characteristics of the combustion noise and relate the sound quality back to the combustion characteristics for combustion diagnosis.

In this paper, based on the analysis of the Wigner-Ville distribution of the overall engine noise, the combustion noise is extracted by using coherent power spectrum analysis and a band-pass filter based on fractional Fourier transform (FRFT), and then the characteristics of the extracted combustion noises are investigated for combustion process monitoring and fuel quality evaluation.

The objectives of this paper are (1) to investigate the relationship between the vibro-acoustic characteristics and combustion process of a CI diesel engine operating with biodiesels; (2) to reflect the combustion characteristics through analysing the characteristics of combustion noise; and (3) to evaluate the fuels quality by analysing the vibro-acoustic characteristics of diesel engines. This paper is organised as follows, the CI engine combustion process and combustion characteristics are presented in section 2. Section 3 introduces the experimental test rig and testing procedure. The analysis results and discussion are detailed in section 4. Finally, the conclusions are summarized in section 5.

2.   CI engine combustion

### 2.1 Combustion characteristics

The combustion process of diesel engines is a complexity process due to the combustion mechanism. The important parameters that signify the combustion characteristics effectiveness are cylinder pressure, ignition time delay, and heat release rate (HRR) .etc. (Enweremadu and Rutto, 2010). The cylinder pressure can be measured from the engine directly, and all the other combustion characteristics are based on the calculation of cylinder pressure. The HRR can be used for identifying the start of combustion, indicating the ignition delay for different fuels, showing the fraction of fuel burned in the premixed mode and differences in combustion rates of fuels (Brunt et al., 1998). And it can be computed from a simplified approach which was derived from the first law of thermodynamics as expressed in Eq. (1).

$$\frac{dQ}{d\theta} = \frac{1}{\gamma-1}\left(\gamma P \frac{dV}{d\theta} + V \frac{dP}{d\theta}\right) \tag{1}$$

where, $dQ/d\theta$ is the heat release rate across the system boundary into the system, P is the in-cylinder pressure, V is the in-cylinder volume, γ which ranges from 1.3 to 1.5 for heat release analysis is the ratio of specific heat, θ is the crank angle. Moreover, $P(dV/d\theta)$ is the rate of work transfer done by the system due to system boundary displacement(Heywood, 1988).

Figure 1 presents the cylinder pressure and HRR of a diesel engine. It indicates that the combustion process can be divided into three distinguishable stages (Zhen et al., 2013). Although the starts of the premixed period and the mixing controlled period are shifted to some extent, the three stages should be determined basically according to the HRR and cylinder pressure curve. The first stage is the premixed period where the rate of burning is very high and the combustion time is short (for only a few crank angle degrees) as well as the cylinder pressure rises rapidly. The second stage is the main heat release period corresponding to a period of gradually decreasing HRR and lasting about

30 crank degrees, namely mixing controlled period. The third stage is the late combustion period which corresponds to the tail of heat release diagram in which a small but distinguishable HRR throughout much of the expansion stroke.
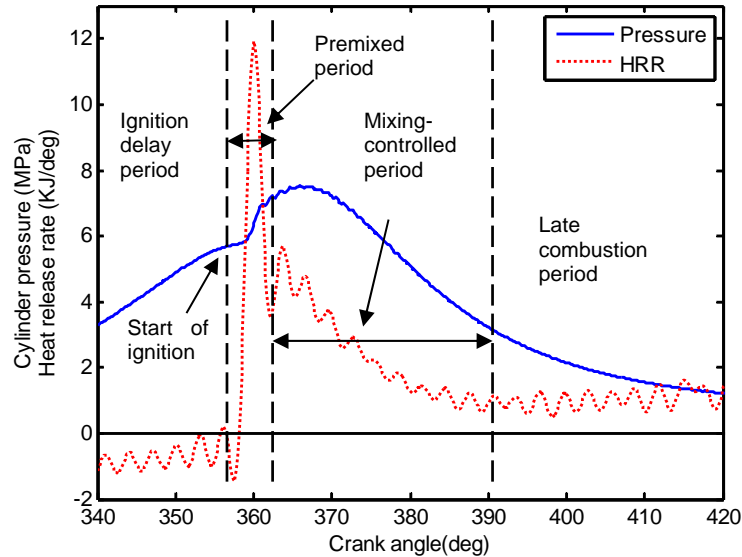

Figure 1. Cylinder pressure and heat release rate of diesel engine

2.2 Combustion Vibration and Noise

Combustion noise is a complex noise whose level and sound quality both strongly depend on the fuel combustion and is one of the main engine noise sources (Pruvost et al., 2009). It occurs towards the end of the compression stroke and subsequent expansion stroke. The rapid pressure changes due to the combustion results in vibration transmitted through engine structures, forms a part of the airborne noise, and contributes to the overall engine noise level. The pressure variation in the engine cylinder plays an important role in the analysis of the combustion characteristics, combustion noise of fuels, and the sound quality related to the combustion process (Pruvost et al., 2009). Therefore, the combustion process and diesel engine fuels could be monitored through analysing the characteristics of combustion noise.

There are three main paths for the vibration and noise transmission based on their generation mechanism and the engine structures (LI, 2000). Figure 2 indicates the three main paths including cylinder head, gas excitation inside cylinder, and mechanical parts (Zhen et al., 2012). The first path begins from the cylinder head to the cylinder block and then directly into the air from the external surfaces. The second path is the gas explosion directly exciting the cylinder block through which the noise is transmitted. The third path initiates from the piston to the connecting rod and then transmits to cylinder block through the crankshaft which can be considered as mechanical induced noise. The gas explosion will excite the cylinder head, cylinder block and piston during the combustion process, and all the combustion noise is radiated to the air through the external surfaces of the engine, and contributed to the overall engine noise.
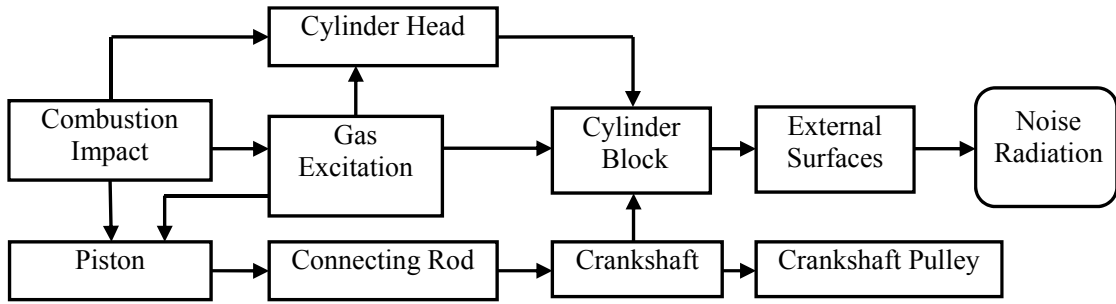
Figure 2. The combustion noise generation diagram

3. Experimental Test rig and Testing Procedure

The experiment was conducted on a test rig which consists of a diesel engine, charge amplifier for vibration signal, filter and amplifier for sound signal, ADC, load, and PC for saving data and analysis. The diesel engine is a four-cylinder, four-stroke, turbocharged, water-cooled, and direct injection. The load for the engine was provided by a 200 kW AC dynamometer with 4 quadrant regenerative drive with monitoring and absorbing capability for both steady and transient conditions. The schematic diagram of the test rig and engine specifications is shown in Figure 3 and Table 1, respectively.
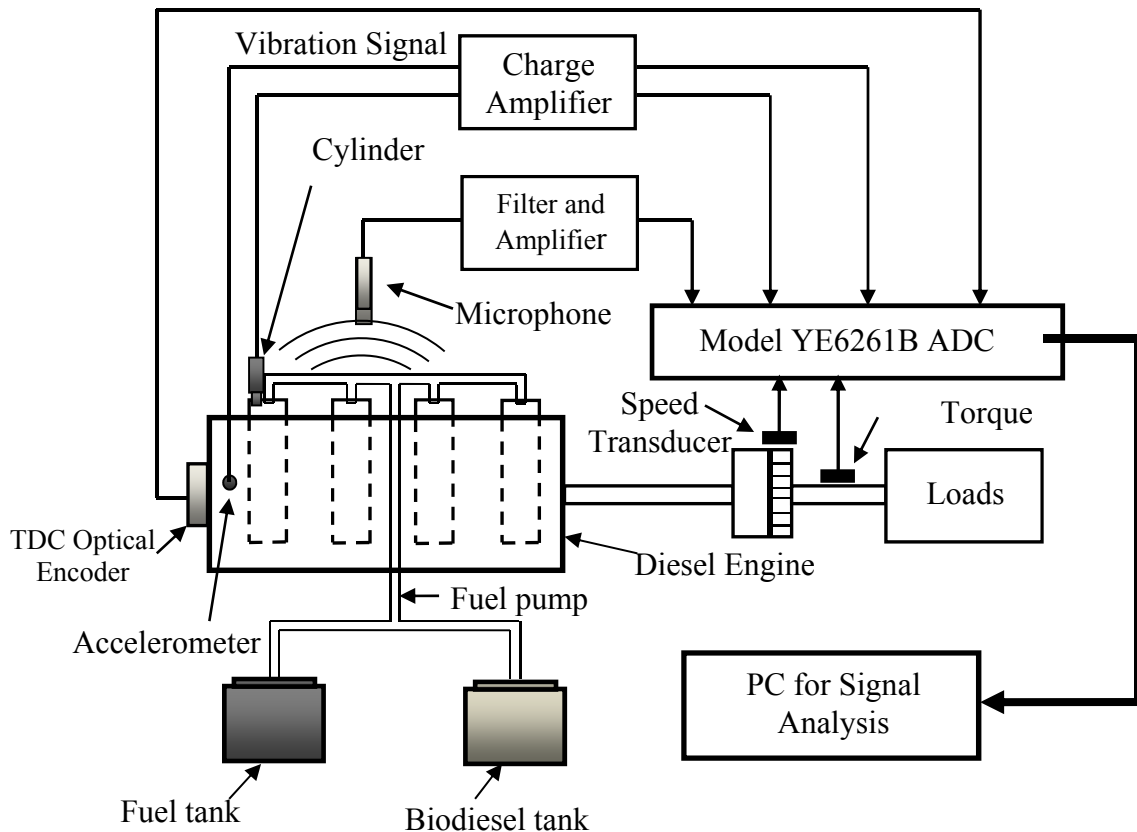
Figure 3. Schematic diagram of test rig

Table 1. Specifications of the test diesel engine

Type of engine	Turbocharged diesel engine
Number of cylinders	4
Bore	103mm
Stroke	132mm
Compression ratio	18.3
Injection system	Direct injection
Displacement	4.399 litre
Cooling system	Water
Maximum power	74.2 kw @ 2200 rpm

In the experiment, the test engine was tested with different fuels and operated at different speeds and loads. Concretely, the test engine was fuelled with rapeseed oil, its blends involved B50 and B100, and pure diesel at the constant speeds of 900rpm, 1100rpm and 1300rpm. B50 is a mixture of 50% rapeseed oil and 50% diesel whilst B100 is 100% rapeseed oil in volume. The loads were varied from 0 to 420Nm with an interval of 105Nm at each constant speed. The details of the operating conditions are given in Table 2.

Table 2. Operating conditions

| Fuel	Speed (rpm)	Load (Nm)
Pure Diesel	900, 1100, 1300	105, 210, 315, 420
B50	900, 1100, 1300	105, 210, 315, 420
B100	900, 1100, 1300	105, 210, 315, 420

During the tests, the engine speed, cylinder pressure, crank angle position, engine vibration and acoustic signals were measured and recorded for future analysis. Engine speed was measured by a Hengler RS58 speed sensor. The cylinder pressure was measured by Kistler 6125A11 model air-cooled Piezo-Quartz pressure sensor that was mounted on the 1st cylinder head. The vibration of the engine body was measured using accelerometers with the sensitivity of $4.9mV/ms^{-2}$. The pressure sensor and accelerometer signals were passed through a B&K type 2635 charge amplifier before feeding them to the Analogue-to-Digital Converter (ADC). The charge amplifier was used to amplify the signals and filter out unwanted signal components (Albarbar et al., 2010). The engine acoustic signal was measured by using BAST's microphone system composed of electrets microphone CHZ-211 and preamplifier YG-201 with the sensitivity of 48.4mV/Pa and frequency response of 6.3Hz-20 kHz. Moreover, crankshaft position was obtained using a crankshaft angle sensor to determine cylinder gas pressure as a function of crank angle.

All the signals collected need to be converted from the analogue form to the digital form so that they were suitable for computer analysis. This can be carried out by using a data acquisition system which is based on the hardware of Model YE6261B dynamic data acquisition equipment. The Model YE6261B consists of 32 channels with 16 bit resolution for each channel, synchronized acquisition at 100 kHz per channel, IEEE 1394 interface selectable signal conditioners.

4.   Results and Discussion

4.1 Cylinder pressure variation

Based on the theoretical analysis in Section 2, the variation of the cylinder pressure is the main characteristics of the combustion process. Cylinder pressure versus crank angle over the compression and expansion strokes of the engine operating cycle can be used to obtain quantitative information on the progress of combustion (Heywood, 1988). Figure 4 shows the cylinder pressures versus crank angle for different fuels (diesel, B50, and B100), and engine loads (105Nm, 210Nm, 315Nm and 420Nm) at a constant engine speed of 1300rpm. Three operating cycles were presented and their patterns are uniform and dependable. It also can be seen that the cylinder pressure peak values are increased according to the increasing of engine loads.
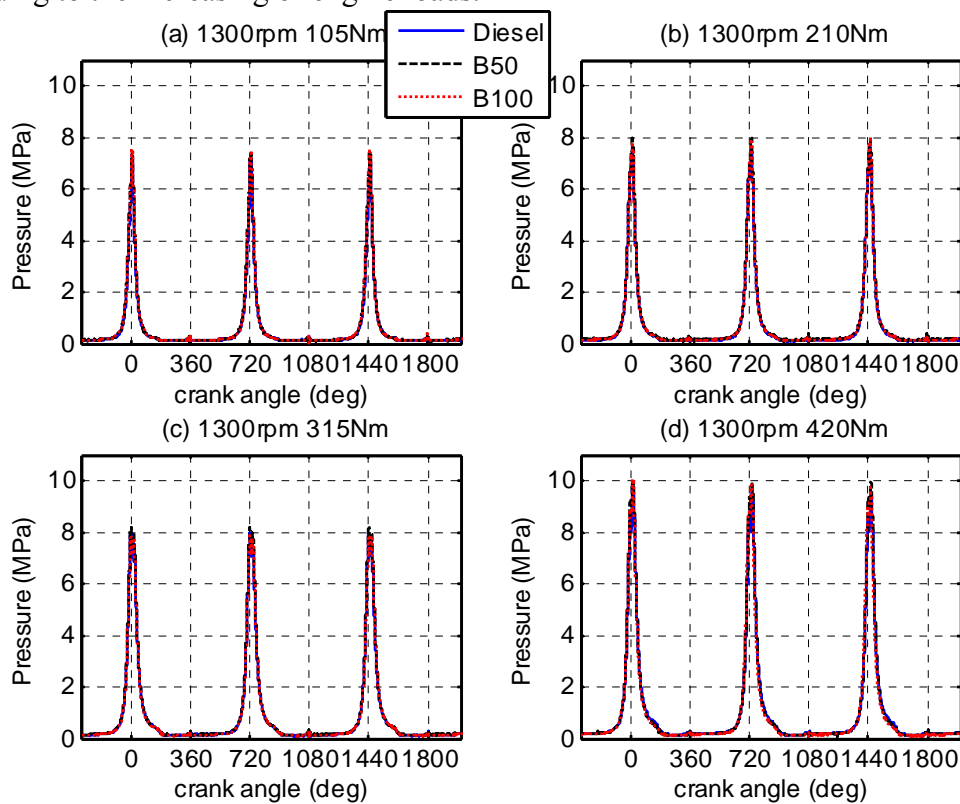

Figure 4. Cylinder pressure at speed of 1300rpm and under different loads

For analysing the variation of cylinder pressure of different supplied fuels, the cylinder pressure signals in one engine operating cycle were zoomed in details and the pressure rising rate was calculated and shown in Figure 5. It can be effortlessly seen that the peak cylinder pressure was higher for rapeseed oil biodiesel at all tests. The higher cylinder pressure of test engine running with biodiesel may be attributed to the higher in-cylinder pressure during the compression strokes the advanced combustion process initiated by the physical properties such as higher cetane number, viscosity, density and bulk modulus (Tesfa et al., 2013). The fuels achieve complete combustion resulting in a higher in-cylinder pressure. Moreover, the higher viscosity of biodiesel can enhance fuel spray penetration and thus improving air-fuel mixing (Lin et al., 2009). Conversely, a higher viscosity of biodiesel can also lead to bad fuel injection atomization. The peak

cylinder pressure of B50 is slightly higher than that of B100, especially in high load. This is possibly because of the higher viscosity of B100. The viscosity of the biodiesel is increased with the increasing of biodiesel percentage in the blends. However, the higher viscosity leads to the decrease of combustion efficiency due to the bad fuel injection atomization (Aydin and Bayindir, 2010).
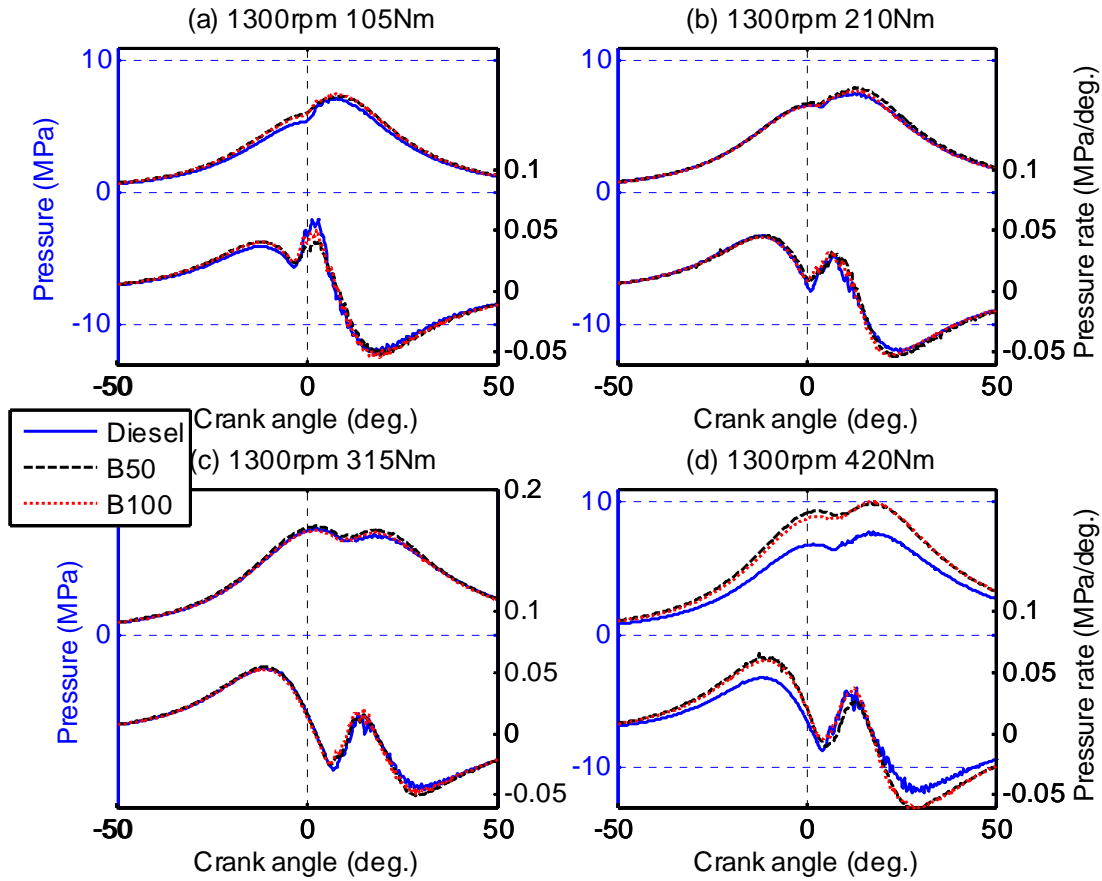
Figure 5. The variation of cylinder pressure and pressure rising rate

For the comparison of cylinder pressure variation, the peak values of the cylinder pressure and pressure rising rate were calculated and shown in Figure 6. Obviously, with the increasing of engine operating loads and speeds, the cylinder pressure peak values for both diesel and biodiesels are slightly increased. Refer to the literature (Gumus, 2010)(Ozsezen et al., 2009)(Canakci et al., 2009)(Meng et al., 2008)(Lapuerta et al., 2005), this maybe because of longer ignition delay results in more fuel available for ignition and more energy release during the premixed combustion stage. Figure 6(b) shows that the peak values of pressure rising rate also follows the same trend with the cylinder pressure peak values in most of the test cases. And the peak values of pressure rising rate for B50 are slightly higher than that for diesel and B100 under the loads of 210 Nm, 315 Nm and 420 Nm. However, the peak values of pressure rising rate present different patterns under the load of 105 Nm. The highest peak value is for diesel, and the lowest is for B50. From Figure 5, it can be seen that the higher peak values of pressure rising rate are generated almost in the premixed combustion stage under the loads of 105 Nm (Figure 5(a)), but others are generated in the ignition delay stage under the loads of 210 Nm, 320 Nm and 420 Nm. In Figure 5(a) under the load of 105 Nm, it

can be found that the highest values rate are for B50 and the lowest values are for B100 from the comparison of the peak values of pressure rising rate in the ignition delay stage. This is consistent with the trend of other three load cases.
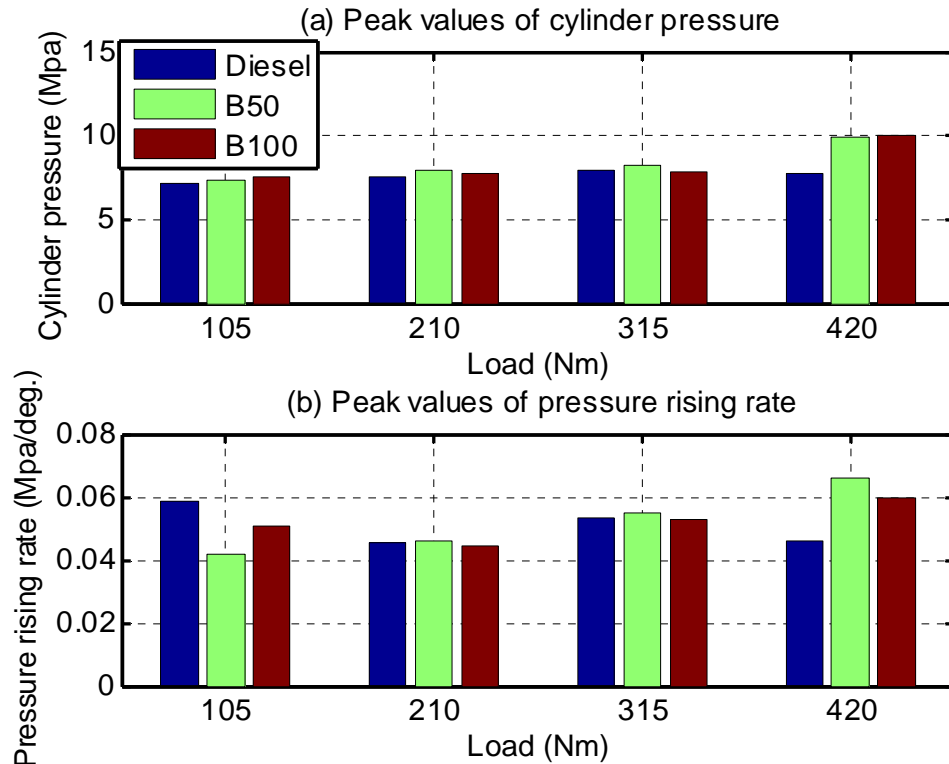

Figure 6. Peak values of cylinder pressure and its rising rate at the speed of 1300rpm

4.2 Vibration and acoustic signals

The vibration and acoustic signals of engines are closely related to the combustion process. Figure 7 shows the acoustic signals upon the monitored body vibration and cylinder pressure in the angular domain. It can be seen that higher cylinder pressure obtained from the combustion process produces higher engine vibration and noise that contributes to the overall engine noise. This indicates that the vibration of cylinder head should be due to the changes of cylinder pressure during the combustion process. The noise produced by the vibration of cylinder head should be related to the combustion process, and can be considered as the main components of the combustion noise. Therefore, the characteristics of combustion process should be reflected through analysing the features of the combustion noise. However, the main point is how to extract the combustion noise from the overall engine noise effectively.

Through analysing the vibro-acoustic characteristics of the diesel engine (Zhen et al., 2013), it found that the amplitudes of engine vibration and acoustic signals are increased in consistent with the increasing of operating loads and speeds under all types of fuels with clear patterns. However, it is difficult to extract effective features for monitoring combustion process and fuels quality from the raw engine noise signals due to the complexity of engine noise sources, transmission paths and the multiply interference between independent sources. Actually, the main noise sources of engine

are the machinery noise and the combustion noise (Shu and Liang, 2007). The engine noise in low-frequency band is the noise of mechanical components e.g. oil pumps, gears, valves, etc. which radiated from thin-walled part such as gear cover and valve cover. The combustion noise is located in the high-frequency band of engine noise which radiated from the combustion process referred to Shu's analysis of engine noise using coherent power spectrum analysis (Shu and Liang, 2007).
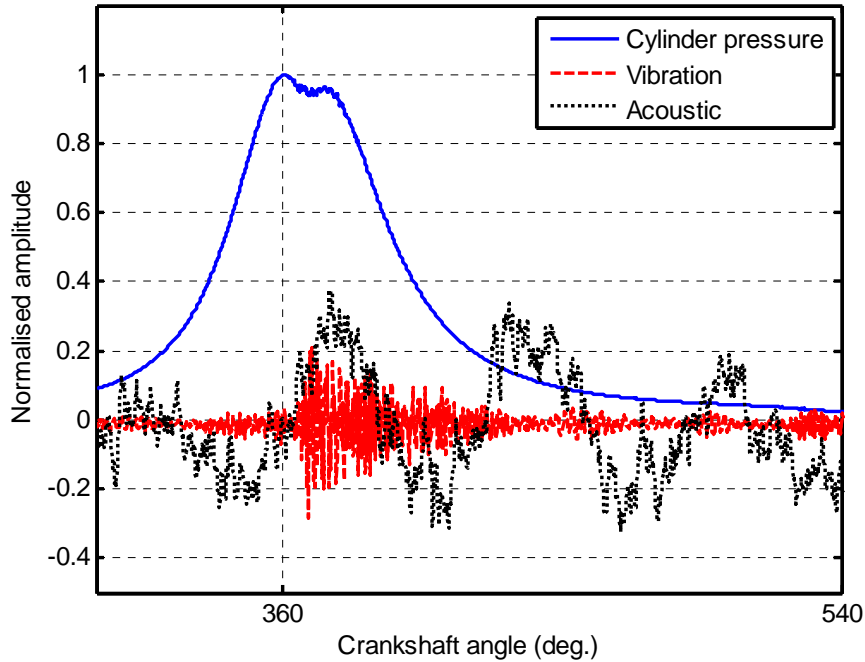

Figure 7. Normalised cylinder pressure, body vibration and engine acoustic

Figures 8 and 9 show the spectrum of vibration and acoustic signals under the low operating condition (900rpm, 105 Nm) and the high operating condition (1300rpm, 420 Nm), respectively. It shows the amplitudes of vibration and acoustic signals increased alongside the increasing of operating loads and speeds. And the amplitudes of the engine noise spectrum are higher in the low-frequency band than that in the high-frequency band. This is potentially because of the resonance of the engine room modes being excited by the test engine noise (LI, 2000). Moreover, the main frequency components of the machinery noise and vibration in the low frequency band are related to the firing frequencies and their harmonics which is consistent with the operating speeds. However, it is also difficult to distinguish the fuels from the spectrum. Based on the generation mechanism of the acoustic signals, engine noise is mainly excited by the vibration of the engine surface which is caused by the in-cylinder pressure variation during the combustion process. Therefore, the characteristics of engine noise should be related to the variation of cylinder pressure and can be used to diagnose the combustion process.
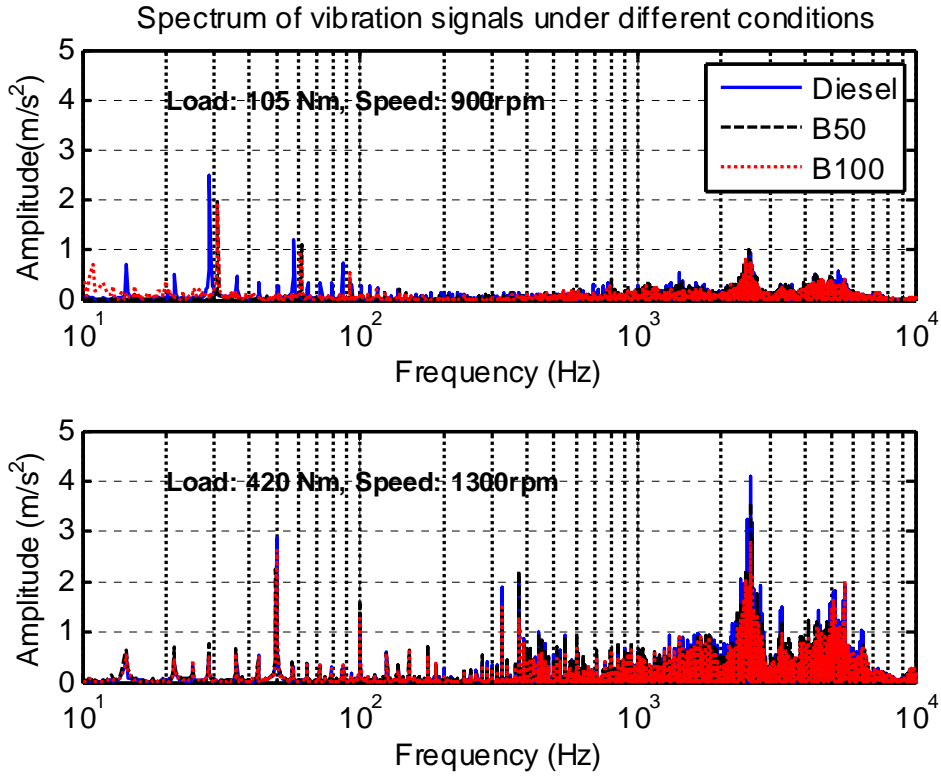
Figure 8. spectrum of vibration signals under different conditions
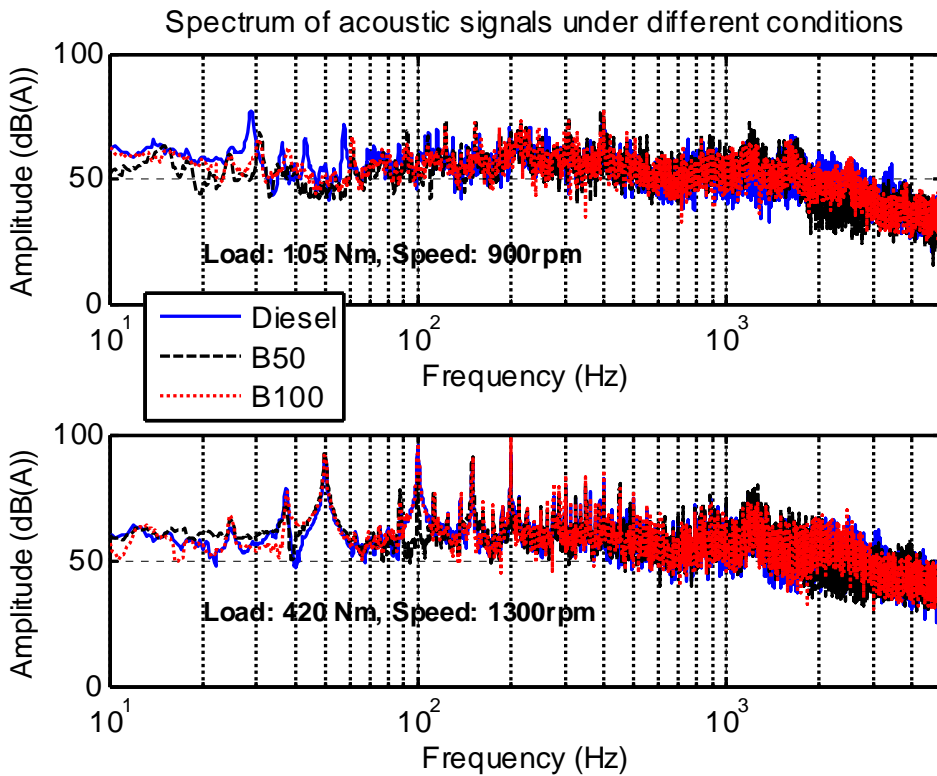
Figure 9. Spectrum of acoustic signals under different conditions
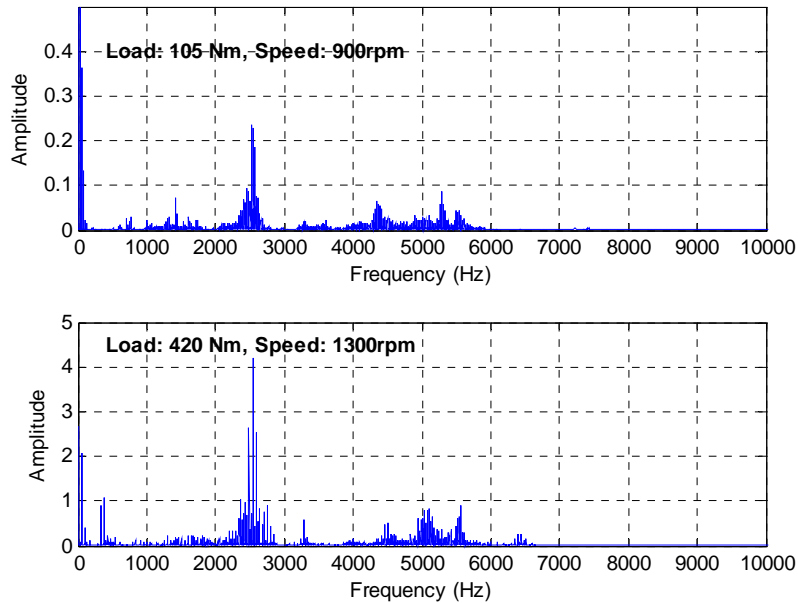
4.3 Coherent power spectrum analysis

For analysing the correlation of the engine noise, cylinder head vibration, and combustion process, the coherent power spectrum (CPS) analysis was employed to identify the noise sources that are related to the combustion process. The input CPS can be defined as the product of the coherent function and the input power spectrum (Shu and Liang, 2007) as shown in Equation (2) and (3),

$$G_{yx}(f) = \gamma_{xy}^2 G_{xx}(f) \qquad (2)$$

and

$$\gamma_{xy}^2 = \frac{|G_{xy}(f)|^2}{G_{xx}(f)G_{yy}(f)} \qquad (3)$$

where x can be considered as the input signal, and y denotes the output signal of measurement system. G_{xx} and G_{yy} are the self-power spectrum of x and y, respectively. G_{xy} is the cross power spectrum between the input signal x and the output y. γ_{xy}^2 represents the coherent function of the input signal x and the output signal y.

Figure 10. Coherent power spectrum analysis of engine noise

In this study, the signal measured by an acceleration sensor located at the cylinder head of the test engine is used as the input signal for the CPS analysis while the output signal is the signal measured by a microphone which is the measured overall engine noise. Figure 10 shows the CPS analysis results under the low and high operating conditions. It indicates the vibration and noise signals related to the combustion process mainly contributes to the engine noise at the frequency band of 2 kHz - 3 kHz. And the amplitudes of the CPS increased together with the increasing of the operating loads and speeds, leading to the increasing of engine noise accordingly.

4.4 Wigner-Ville distribution of engine noise

Before extracting the engine noise that related to the combustion process, the Wigner-Ville distribution (WVD) was used to analyse the measured engine noise in order to demonstrate the time-frequency distribution characteristics of the measured overall engine noise. The continuous WVD of a general signal $x(t)$ can be defined by Equation (4) (Matz and Hlawatsch, 2003).

$$W_f(t,\omega) = \int_{-\infty}^{+\infty} x(t+\tau/2)\,x(t-\tau/2)e^{-j\omega\tau}d\tau \tag{4}$$

where $x(t)$ is the real-valued time signal and t and ω are the time and frequency indices, respectively. τ is the redius extending from time t. However, from the Equation (4), the instantaneous power relies on the nature of the signal far away from the time t due to the integral requiring an infinite signal length. As a result, the localisation characteristics of the WVD are reduced to some extent. In application, a time window $w(t)$ is often added to the analysed signal before the transformation is carried out.

$$x_w(t) = x(t)w(t) \tag{5}$$

The length of the added window in Equation (5) is much shorter than that of the analytical signal. The window has the ability to slide along the time axis so that its centre is always located at time t. This short-timed window capably makes the transformation of capturing transients with a better resolution. In this paper, the Choi-Williams (CW) window was applied. The WVD of the windowed signal as shown in Equation (5) can be expressed as follow:

$$W_{f_w}(t,\omega) = \frac{1}{2\pi}\int_{-\infty}^{+\infty} W_f(t,\eta)\,W_{cw}(t,\omega-\eta)d\eta$$

$$= \frac{1}{2\pi}\int_{-\infty}^{+\infty} W_f(t,\eta)\exp[-\frac{(2\pi t(\omega-\eta))^2}{\sigma}]d\eta \tag{6}$$

where W_f and W_{cw} are the WVD of the analytical signal and the CW window function, respectively. And σ is a positive parameter controlling the concentration of W_{cw} around the origin of the (t,ω) plane(Hlawatsch et al., 1995). In this paper, $\sigma = 0.05$ was selected for analysing the measured engine acoustic signals.

Figure 11 shows the WVD of the overall engine noise for different supplied fuels under the loads of 105Nm and 420Nm (900rpm). The length of the window for the WVD is determined based on one complete combustion cycle (720 degrees). It can be seen that the main energy of the engine noise is located in the low frequency band which is below 1 kHz under the low engine load of 105Nm as shown in Figure 11 (a), (c) and (e). And the engine noise energy also changes alongside the increasing of the biodiesel percentage at the high frequency band of 2 kHz-3 kHz. Meanwhile, the similar conclusions can be obtained through analysing the WVD of engine noise under the high load of 420 Nm as shown in Figure 11 (b), (d) and (f). This variation can be used to distinguish the fuel types through analysing the engine noise distribution. Moreover, based on the analysis of the relationship between engine vibration and engine noise in

section 4.3, the main frequency band of the overall engine noise that related to the combustion process is from 2 kHz to 3 kHz. Therefore, it seems that the engine noise that located at the frequency band of 2 kHz-3 kHz can be used for monitoring the combustion process and the engine supplied fuels.
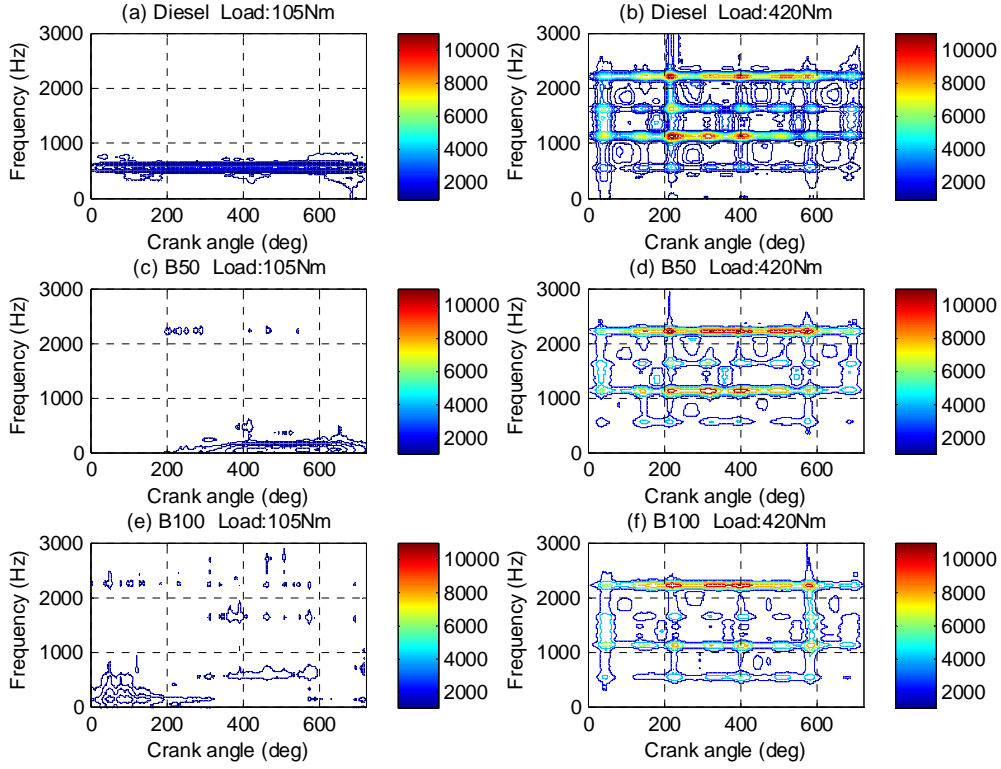
Figure 11. WVD of engine noise at loads of 105Nm and 420Nm

4.5 Combustion noise extraction

For extraction the main component of the combustion noise, a filter based on fractional Fourier transform (FRFT) is designed to process the measured overall engine noise. The FRFT is a time-frequency distribution extended from the classical Fourier transform (FT). FRFT is a technique which rotates the conventional time-frequency domains to a specified angle α allowing the designer to have more flexibility for extracting the useful signals or decreasing noisy signals (Ozaktas et al., 1996). The αth order FRFT of a signal $x(t)$ can be defined as (Sejdić et al., 2011)

$$X_p(u) = \int_{-\infty}^{+\infty} x(t)K_p(t,u)dt \tag{7}$$

$$\alpha = p\frac{\pi}{2} \tag{8}$$

where u denotes the variable in the αth-order fractional Fourier domain, which is the frequency for conventional Fourier transform with a kernel function $K_p(t, u)$, and p is the represent of the order α of the fractional Fourier transform.

$$K_p(t,u) = \begin{cases} \sqrt{\dfrac{1-jcot\alpha}{2}} e^{j(\frac{1}{2}u^2 cot\alpha+\frac{1}{2}t^2 cot\alpha-utcsc\alpha)}, & \alpha \neq n\pi \\ \delta(t-u), & \alpha = 2n\pi \\ \delta(t+u), & \alpha = (2n+1)\pi \end{cases} \quad (9)$$

It is found that the FRFT of the signal $x(t)$ at the order $\alpha = 0$ is the input signal itself $x(t)$; at the order $\alpha = \pi/2$ corresponds to the FT of the signal $x(t)$; and at the order $\alpha = \pi$ is the inverse of the signal $x(-t)$.

The filtering process based on FRFT is described as follows (Sejdić et al., 2011)(Ozaktas et al., 1996).

1. Calculation of the FRFT of the analytical signal according to the variation of the order α. The range of p is chosen from 0.5 to 1.5. The energy distribution of the analytical signal on the fractional plane can be obtained as shown in Figure 12 (a).

2. Search for the peak point (p_0, u_0) on the fractional plane. Then, calculate the FRFT of the analytical signal at the order of $\alpha_0 = p_0 \dfrac{\pi}{2}$.

3. Filter the analytical signal in the fractional domain using a band-pass filter. The centre frequency of the filter is based on the localization of the peak point u_0 on the fractional plane. The energy distribution of the filtered signal on the fractional plane is shown in Figure 12 (b).

4. Calculate the FRFT of the filtered signal at the order of $a_0 = -p_0 \dfrac{\pi}{2}$ to obtain the extracted signal in the time domain.
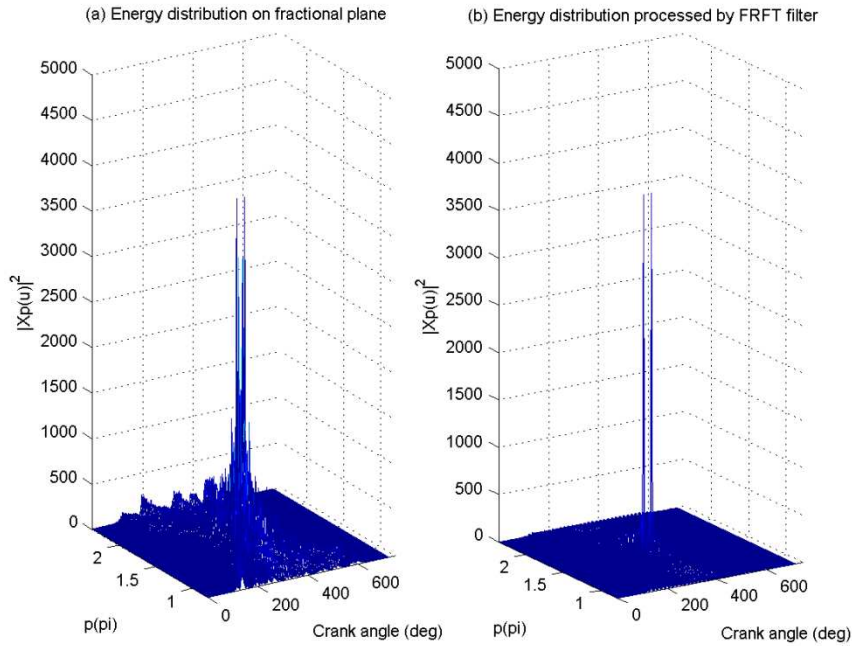

Figure 12. An example of energy distributions on the fractional plane
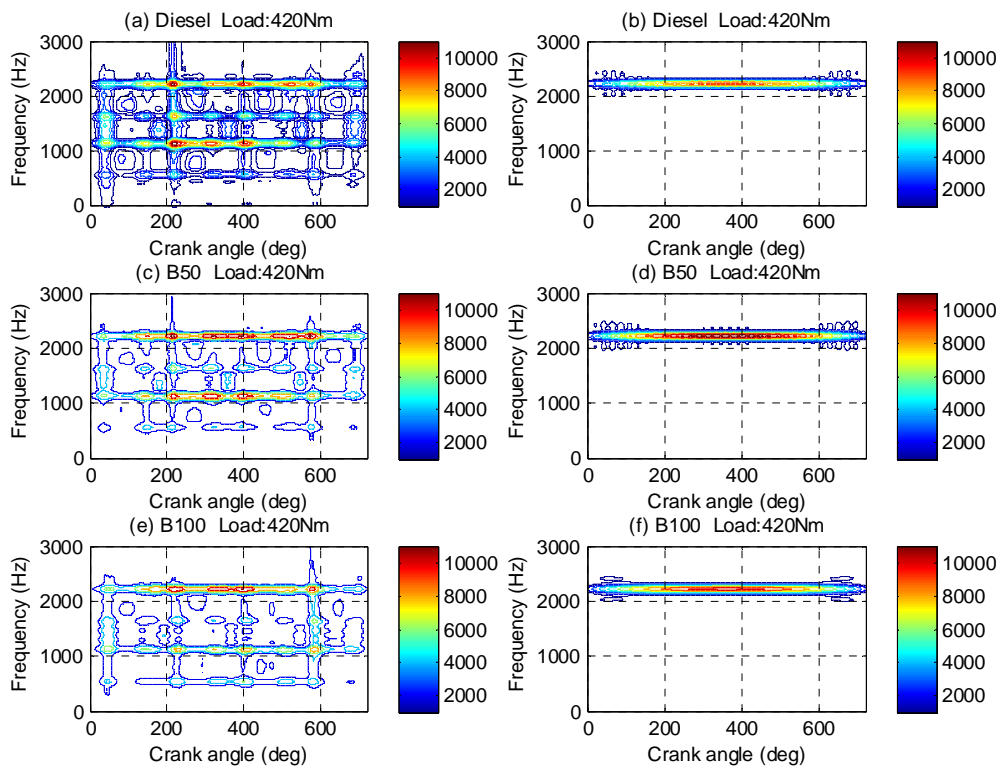
Figure 13. WVD of engine noise processed by FRFT filter

The WVD of the main component of the combustion noise that extracted using the band-pass filter based on FRFT is shown in Figure 13 (b), (d) and (f). For the comparison, Figure 13 (a), (c) and (e) show the WVD of the unfiltered engine noise at the load of 420Nm for different supplied fuels. It is clear that the combustion related noise from 2 kHz to 3 kHz was extracted from the overall engine noise by applying the band-pass filter. For designing a linear indicator to distinguish the fuels and monitor the combustion process, the standard deviation of sound pressure levels (SPLs) of the extracted combustion noise were calculation for different operation conditions as shown in Figure 14. It shows that the SPLs are increased together with the increasing of operating speeds and loads for all fuels. And it can also identify the differences between different fuels. In details, the SPLs of the extracted combustion noise of the test engine fuelled with biodiesel (B50 and B100) are slightly higher than that fuelled with diesel. And the SPLs of the extracted combustion noise of the test engine fuelled by B50 are higher than that fuelled by B100 under all test cases. This is consistent with the variation of cylinder pressure rising rate in most of the test cases as shown in Figure 6. Therefore, the research results presented that the characteristics of combustion noise can be used to reflect the variation of the engine combustion process and the fuel quality also can be monitored and evaluated.
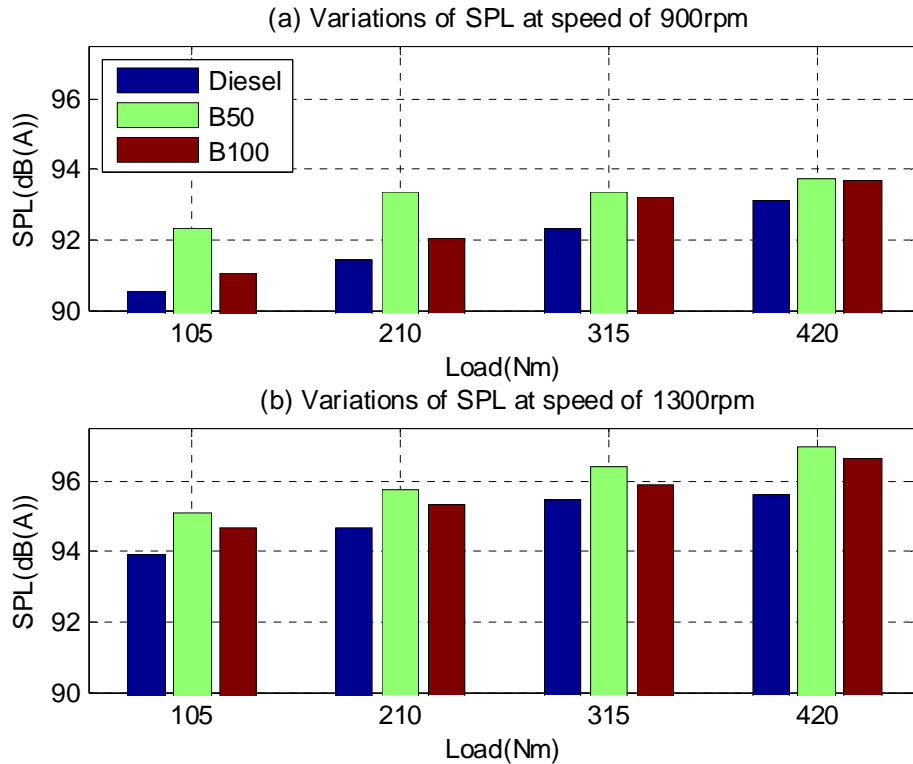
Figure 14. Variations of SPLs under different operating conditions

5. Conclusion

This paper carried out an experimental investigation on the combustion, cylinder head vibration, and noise analysis of a CI diesel engine operating with rapeseed biodiesels under steady state operating conditions. Based on the experimental study, the main results are summarized as follows:

- The cylinder pressure and its rising rate for biodiesel are higher than that for diesel at most of the test cases. And their peak values increased with the increasing of operating loads and speeds.
- The amplitudes of the engine vibration and acoustic signals increased alongside the engine loads and speeds.
- The proposed filter based on FRFT is an effective tool that can be used to extract the main component of the combustion noise.
- The SPLs of the extracted combustion noise are slightly higher when the test engine fuelled by biodiesels.
- The features of the combustion noise can be used to reflect the combustion characteristics and evaluate the fuel quality.

Acknowledgments

References

Albarbar, A., Gu, F., Ball, A.D., Starr, A., 2010. Acoustic monitoring of engine fuel injection based on adaptive filtering techniques. Appl. Acoust. 71, 1132–1141. doi:10.1016/j.apacoust.2010.07.001

Aydin, H., Bayindir, H., 2010. Performance and emission analysis of cottonseed oil methyl ester in a diesel engine. Renew. Energy 35, 588–592. doi:10.1016/j.renene.2009.08.009

Brunt, M.F.J., Rai, H., Emtage, A.L., 1998. The Calculation of Heat Release Energy from Engine Cylinder Pressure Data (No. 981052). SAE International, Warrendale, PA.

Canakci, M., Ozsezen, A.N., Turkcan, A., 2009. Combustion analysis of preheated crude sunflower oil in an IDI diesel engine. Biomass Bioenergy 33, 760–767. doi:10.1016/j.biombioe.2008.11.003

Dorado, M.., Ballesteros, E., Arnal, J.., Gómez, J., López, F.., 2003. Exhaust emissions from a Diesel engine fueled with transesterified waste olive oil☆. Fuel 82, 1311–1315. doi:10.1016/S0016-2361(03)00034-6

Enweremadu, C.C., Rutto, H.L., 2010. Combustion, emission and engine performance characteristics of used cooking oil biodiesel—A review. Renew. Sustain. Energy Rev. 14, 2863–2873. doi:10.1016/j.rser.2010.07.036

Gumus, M., 2010. A comprehensive experimental investigation of combustion and heat release characteristics of a biodiesel (hazelnut kernel oil methyl ester) fueled direct injection compression ignition engine. Fuel 89, 2802–2814. doi:10.1016/j.fuel.2010.01.035

Hamasaki, K., Kinoshita, E., Tajima, S., Takasaki, K., Morita, D., 2001. Combustion characteristics of diesel engines with waste vegetable oil methyl ester. Presented at the The 5th International Symposium on Diagnostics and Modelling of Combustion in Internal Combustion Engines.

Hazar, H., 2009. Effects of biodiesel on a low heat loss diesel engine. Renew. Energy 34, 1533–1537. doi:10.1016/j.renene.2008.11.008

Heywood, J., 1988. Internal combustion engine fundamentals, McGraw-Hill series in mechanical engineering.

Hlawatsch, F., Manickam, T.G., Urbanke, R.L., Jones, W., 1995. Smoothed pseudo-Wigner distribution, Choi-Williams distribution, and cone-kernel representation: Ambiguity-domain analysis and experimental comparison. Signal Process. 43, 149–168. doi:10.1016/0165-1684(94)00150-X

Kjärstad, J., Johnsson, F., 2009. Resources and future supply of oil. Energy Policy 37, 441–464. doi:10.1016/j.enpol.2008.09.056

Lapuerta, M., Armas, O., Ballesteros, R., Fernández, J., 2005. Diesel emissions from biofuels derived from Spanish potential vegetable oils. Fuel 84, 773–780. doi:10.1016/j.fuel.2004.11.010

Lin, B.-F., Huang, J.-H., Huang, D.-Y., 2009. Experimental study of the effects of vegetable oil methyl ester on DI diesel engine performance characteristics and pollutant emissions. Fuel 88, 1779–1785. doi:10.1016/j.fuel.2009.04.006

LI, W., 2000. A STUDY OF DIESEL ENGINE ACOUSTIC CHARACTERISTICS. PhD thesis.

LI, W., GU, F., BALL, A.D., LEUNG, A.Y.T., PHIPPS, C.E., 2001. A STUDY OF THE NOISE FROM DIESEL ENGINES USING THE INDEPENDENT COMPONENT ANALYSIS. Mech. Syst. Signal Process. 15, 1165–1184. doi:10.1006/mssp.2000.1366

Matz, G., Hlawatsch, F., 2003. Wigner distributions (nearly) everywhere: time–frequency analysis of signals, systems, random processes, signal spaces, and frames. Signal Process. 83, 1355–1378. doi:10.1016/S0165-1684(03)00086-0

Meng, X., Chen, G., Wang, Y., 2008. Biodiesel production from waste cooking oil via alkali catalyst and its engine test. Fuel Process. Technol. 89, 851–857. doi:10.1016/j.fuproc.2008.02.006

Murillo, S., Míguez, J.L., Porteiro, J., Granada, E., Morán, J.C., 2007. Performance and exhaust emissions in the use of biodiesel in outboard diesel engines. Fuel 86, 1765–1771. doi:10.1016/j.fuel.2006.11.031

Ozaktas, H.M., Arikan, O., Kutay, M.A., Bozdagt, G., 1996. Digital computation of the fractional Fourier transform. Signal Process. IEEE Trans. On 44, 2141 –2150. doi:10.1109/78.536672

Ozsezen, A.N., Canakci, M., Turkcan, A., Sayin, C., 2009. Performance and combustion characteristics of a DI diesel engine fueled with waste palm oil and canola oil methyl esters. Fuel 88, 629–636. doi:10.1016/j.fuel.2008.09.023

Priede, T., 1980. In Search of Origins of Engine Noise - an Historical Review (No. 800534). SAE International, Warrendale, PA.

Priede, T., 1979. Problems and Developments in Automotive Engine Noise Research (No. 790205). SAE International, Warrendale, PA.

Pruvost, L., Leclère, Q., Parizet, E., 2009. Diesel engine combustion and mechanical noise separation using an improved spectrofilter. Mech. Syst. Signal Process. 23, 2072–2087. doi:10.1016/j.ymssp.2009.04.001

Ra, Y., Yun, J.E., Reitz, D., n.d. NUMERICAL PARAMETRIC STUDY OF DIESEL ENGINE OPERATION WITH GASOLINE. Combust. Sci. Technol. 181, 350–378.

Sejdić, E., Djurović, I., Stanković, Lj., 2011. Fractional Fourier transform as a signal processing tool: An overview of recent developments. Signal Process., Fourier Related Transforms for Non-Stationary Signals 91, 1351–1369. doi:10.1016/j.sigpro.2010.10.008

Shu, G., Liang, X., 2007. Identification of complex diesel engine noise sources based on coherent power spectrum analysis. Mech. Syst. Signal Process. 21, 405–416. doi:10.1016/j.ymssp.2006.06.001

Shu, G., Wei, H., Han, R., 2004. Separate the noise of piston slapping from the combustion noise of the internal combustion engine. Presented at the Proceedings of the 33th Inter-Noise, Prague, Czech Republic.

Sudhir, C.V., Sharma, N.Y., Mohanan, P., 2007. Potential of waste cooking oils as biodiesel feedstock. Emir. J Eng Res 12, 69–75.

Tesfa, B., Mishra, R., Gu, F., Ball, A.D., 2012. Water injection effects on the performance and emission characteristics of a CI engine operating with biodiesel. Renew. Energy 37, 333–344. doi:10.1016/j.renene.2011.06.035

Tesfa, B., Mishra, R., Zhang, C., Gu, F., Ball, A.D., 2013. Combustion and performance characteristics of CI (compression ignition) engine running with biodiesel. Energy 51, 101–115. doi:10.1016/j.energy.2013.01.010

Zhen, D., Tesfa, B., Yuan, X., Wang, R., Gu, F., Ball, A.D., 2012. An investigation of the acoustic characteristics of a compression ignition engine operating with biodiesel blends. J. Phys. Conf. Ser. 364, 012015. doi:10.1088/1742-6596/364/1/012015

Zhen, D., Wang, T., Gu, F., Tesfa, B., Ball, A., 2013. Acoustic measurements for the combustion diagnosis of diesel engines fuelled with biodiesels. Meas. Sci. Technol. 24, 055005. doi:10.1088/0957-0233/24/5/055005